ARTICLES

Dissecting a circuit for olfactory behaviour in *Caenorhabditis elegans*

Sreekanth H. Chalasani[1], Nikos Chronis[1], Makoto Tsunozaki[1], Jesse M. Gray[1], Daniel Ramot[2], Miriam B. Goodman[2] & Cornelia I. Bargmann[1]

Although many properties of the nervous system are shared among animals and systems, it is not known whether different neuronal circuits use common strategies to guide behaviour. Here we characterize information processing by *Caenorhabditis elegans* olfactory neurons (AWC) and interneurons (AIB and AIY) that control food- and odour-evoked behaviours. Using calcium imaging and mutations that affect specific neuronal connections, we show that AWC neurons are activated by odour removal and activate the AIB interneurons through AMPA-type glutamate receptors. The level of calcium in AIB interneurons is elevated for several minutes after odour removal, a neuronal correlate to the prolonged behavioural response to odour withdrawal. The AWC neuron inhibits AIY interneurons through glutamate-gated chloride channels; odour presentation relieves this inhibition and results in activation of AIY interneurons. The opposite regulation of AIY and AIB interneurons generates a coordinated behavioural response. Information processing by this circuit resembles information flow from vertebrate photoreceptors to 'OFF' bipolar and 'ON' bipolar neurons, indicating a conserved or convergent strategy for sensory information processing.

Neural circuits actively transform sensory signals: they extract the most relevant sensory information from the environment, determine whether stimuli are increasing or decreasing, and use this information to regulate behaviours on timescales from seconds to hours. It has been suggested that a few connected neurons in statistically over-represented synaptic 'motifs' could perform simple circuit computations[1]. The potential to analyse circuit function at single-cell resolution exists in the nematode *C. elegans*, the nervous system of which contains just 302 neurons with known synaptic connections[2–4]. Functions for many individual *C. elegans* neurons have been inferred from cell ablation studies, chronic activation or recording of neuronal activity[5–10]. However, little has been done to study the dynamic flow of information between neurons—an essential link between circuits and behaviour.

In some *C. elegans* behaviours, sensory inputs lead to long-lasting and complex behavioural sequences. During chemotaxis to food odours or tastes, animals reach an attractant source by regulating turns over many minutes[5,11]. In another food-related behaviour called local search or area-restricted search, animals that have recently been removed from food spend about 15 min exploring a restricted area by interrupting long forward movements with stochastic turns, and then disperse by suppressing turning[12–15]. A pair of olfactory neurons called AWC is important in both of these food-seeking behaviours: the AWC neurons direct chemotaxis to many attractive odours[5], and also increase turning probability during local search[14]. The AWC neurons synapse onto several interneurons including AIB and AIY, which enhance and suppress turning, respectively[13,14] (Fig. 1a). Although the sensory signalling of the AWC neuron has been extensively characterized at a genetic level, nothing is known about the effects of odours on AWC neuron activity, or the mechanisms by which the AWC neuron communicates with downstream neurons. Here we analyse the functional connectivity between the AWC, AIB and AIY neurons that initiates the transformation of chemosensory cues into behaviour.

AWC neurons respond to odour removal

To monitor the odour response of AWC neurons, we used AWC-selective promoters to express G-CaMP, a genetically encoded calcium sensor, the fluorescence intensity of which increases on calcium binding in the physiological range[16,17]. *C. elegans* neurons have rapidly activating voltage-gated calcium channels, suggesting that calcium transients should correlate with strong neuronal depolarization[9,18]. A custom-designed microfluidic device fabricated from the transparent polymer polydimethylsiloxane was used to trap and stimulate animals expressing G-CaMP in one of the two AWC neurons, AWC^{ON} (Fig. 1b–d)[19]. The device restrained *z*-plane movement of the animal so that the AWC neuron remained in focus for imaging, while allowing limited movement in the *x*–*y* plane. Fluid streams under laminar flow were used to deliver the buffer or odour stimuli to the animal's nose. Buffer exchange controls ($n = 18$) showed that short-motion transients, photobleaching and other measurement errors contributed $\Delta F/F$ (fluorescence change/baseline fluorescence intensity) signals $<25\%$ to individual traces, and $<10\%$ to averaged traces (Supplementary Figs 1–3); averaged traces were used for quantification and statistical analysis (Supplementary Fig. 2).

Individual animals were followed in a paired odour addition–odour removal sequence (Fig. 1e, f). Presentation of the attractive odour isoamyl alcohol diminished G-CaMP fluorescence in the AWC^{ON} cell body; although slight, the decrease was significant when averaged over multiple trials (Fig. 1e, h and Supplementary Figs 1–3). Large increases in G-CaMP fluorescence were reliably observed within one second when isoamyl alcohol was replaced with buffer, suggesting an increase in AWC^{ON} calcium on odour removal (an odour-OFF response) (Fig. 1f, i, Supplementary Fig. 1b and Supplementary Movie 1). Increases in G-CaMP fluorescence in AWC^{ON} were also observed when bacteria-conditioned medium was removed from the animal's nose (Fig. 1g and Supplementary Fig. 1h). The AWC^{ON} odour-OFF response was observed at isoamyl alcohol dilutions of 10^{-7} to 10^{-3}, with a maximal response at 10^{-4}

[1]Howard Hughes Medical Institute, Laboratory of Neural Circuits and Behaviour, The Rockefeller University, New York, New York 10065, USA. [2]Program in Neurobiology and Department of Molecular and Cellular Physiology, Stanford University, Stanford, California 94305, USA.

(Fig. 2a); inhibition by odour was maximal at 10^{-5} to 10^{-4} dilution (Supplementary Figs 2 and 3). Chemotaxis to isoamyl alcohol saturates when the odour is uniformly added to agar at $\sim 10^{-4}$ dilution, approximately matching the saturation of the AWC^{ON} calcium response[20,21].

Single *C. elegans* olfactory neurons express multiple G-protein-coupled receptors and sense multiple odours[5]. The AWC^{ON} neuron senses benzaldehyde as well as isoamyl alcohol, and an odour-OFF response was observed in AWC^{ON} across 10^{-6} to 10^{-4} dilutions of benzaldehyde (Fig. 2b). The contralateral AWC^{OFF} neuron also showed odour-OFF G-CaMP responses to isoamyl alcohol and benzaldehyde—a result consistent with behavioural evidence that both AWC^{ON} and AWC^{OFF} sense these two attractive odours[22] (Fig. 2c, d). At low dilutions, the odour 2,3-pentanedione is sensed by AWC^{OFF} and not by AWC^{ON} in behavioural assays, and similarly AWC^{OFF} responded to 2,3-pentanedione at 10^{-7} dilution whereas AWC^{ON} did not (Fig. 2e). In all cases, odour removal increased G-CaMP fluorescence, and odour addition diminished fluorescence.

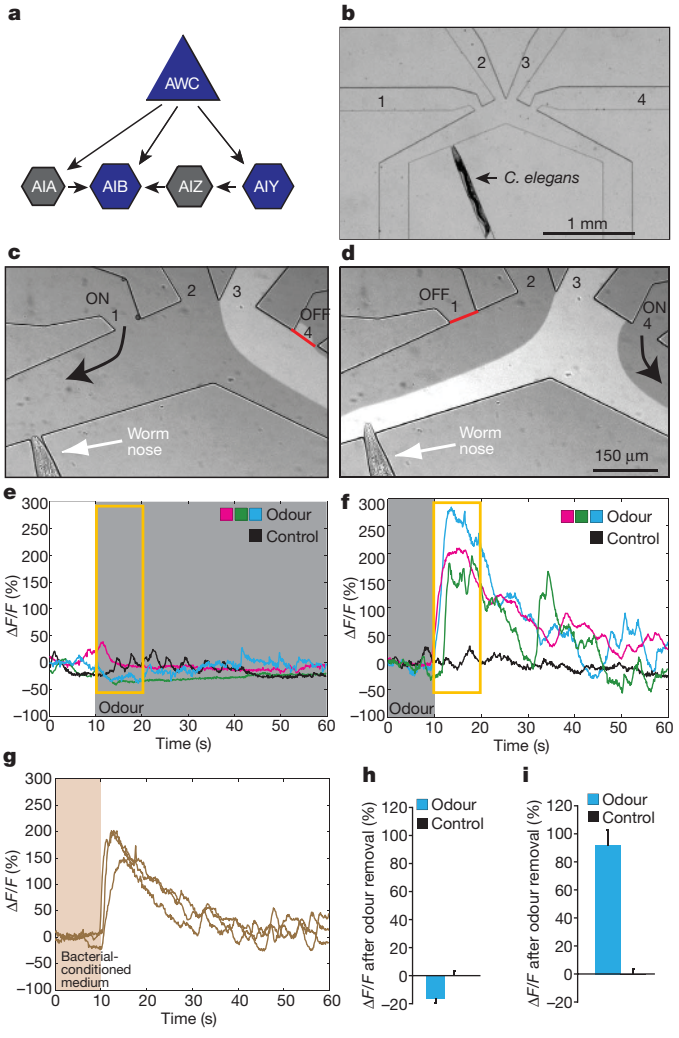

Figure 1 | AWC responds to odour removal. **a**, AWC sensory neurons and downstream interneurons. **b**, Low magnification and **c**, **d**, high magnification view of the PDMS imaging chip, with worm nose exposed to buffer (**c**, streams 1–3 are open; stream 2 reaches the nose) or odour (**d**, streams 2–4 are open; stream 3 reaches the nose). **e**–**g**, Representative G-CaMP responses from AWC^{ON}. **e**, **f**, AWC^{ON} responses on addition (**e**) or removal (**f**) of isoamyl alcohol odour (coloured traces) or buffer (black traces) at 10 s. Grey shading denotes presence of odour; yellow intervals are analysed in **h** and **i**. **g**, AWC^{ON} responses on removal of bacterial-conditioned medium at 10 s. **h**, **i**, Average fluorescence change in AWC^{ON} during the 10 s after odour addition (**h**) or removal (**i**) ($n = 30$). Error bars indicate standard error of the mean (s.e.m.).

The strong bilateral AWC response to 10^{-4} isoamyl alcohol, which resembled the response to bacterial-conditioned medium, was used for subsequent characterization. The AWC^{ON} odour-OFF response was long-lasting, with an average half-time of $\sim$20 s and large secondary peaks throughout the 50 s recording period that were not observed in the presence of odour (Supplementary Fig. 1a), in buffer controls (Supplementary Fig. 1c, d) or with calcium-insensitive green-fluorescent protein (Supplementary Fig. 1e, f). Increasing the duration of odour pre-exposure from 1 to 5 min resulted in a graded odour-OFF calcium response, with a stronger response after longer odour exposure (Fig. 2f). Odour-OFF responses were silenced when isoamyl alcohol was added back after 10 s or 30 s (Fig. 2g, h). Removal of isoamyl alcohol 20 s later elicited a second odour-OFF calcium response of smaller magnitude (42–46% $\pm$ 14% compared to the first response, Fig. 2g, h), suggesting that AWC integrates odour history over $>$20 s. These results suggest that AWC neurons are inhibited by attractive odours, and depolarize when odours are removed, with a response that integrates the concentration and duration of odour exposure.

Odour responses in AIB and AIY interneurons

The AIB and AIY interneurons receive synapses from the AWC neurons, and function with the AWC neurons in local search behaviour[3,13,14] (Fig. 1a). AIB and AIY responses to odours were monitored in the microfluidic device using transgenic lines that expressed G-CaMP under cell-selective promoters. Like AWC, the AIB cell body responded strongly to odour removal with increased calcium, and was inhibited by odour addition (Fig. 3a, b, Supplementary Figs 3 and 4a, b and Supplementary Movie 2). AIB responses were eliminated in animals in which the AWC sensory neurons were ablated (Fig. 3b and Supplementary Fig. 4c, d). These results indicate that the AWC neurons activate AIB interneurons on odour removal.

AIB calcium responses were sustained compared to AWC responses, persisting at near-peak levels for at least 2 min after odour removal (Fig. 3b and data not shown). Two possible explanations, not mutually exclusive, could account for this persistent activity: the AIB interneurons might respond to persistent transmitter release from AWC neurons during the late phase of the response, or AIB interneurons might remain active without AWC input through intrinsic persistent activity or reverberant circuit activity[23]. To examine the first possibility, we removed odour to activate AIB interneurons and then provided odour 30 s later during the period of sustained AIB activity. AIB responses decayed after odour addition, suggesting that AWC neurons continued to stimulate AIB interneurons by releasing transmitter after the end of the strong AWC calcium response (Fig. 3c and Supplementary Fig. 4e, f). This conclusion about AWC is consistent with the known property of nematode (*Ascaris*) motor neurons, which release neurotransmitter in a graded fashion[24].

Like AWC neurons, the AIB interneurons had a graded calcium response to the duration of odour exposure, with longer and stronger responses after 5 min of odour pre-exposure compared to 3 min or 1 min (Fig. 3d).

In AIY neurons, changes in G-CaMP fluorescence were detected in the neurite but not in the cell body; similar observations have been made using temperature stimuli and the cameleon calcium sensor in AIY neurons[25]. In contrast with AWC and AIB neurons, increases in AIY calcium were observed on odour addition and decreases were observed on odour removal (Fig. 3e, f, Supplementary Figs 3 and 5a, b and Supplementary Movie 3). AIY responses were brief, poorly synchronized to odour onset, and appeared sporadically throughout the period of odour presentation (Fig. 3e and Supplementary Fig. 5a). Ablation of the AWC neurons eliminated the AIY response (Fig. 3e, f and Supplementary Fig. 5c, d). These results indicate that AIY is inhibited by AWC, even at the resting level of AWC activity, and that release from this inhibition on odour presentation results in AIY activation.

Thus, AWC, AIB and AIY neurons have distinct dynamic responses to odours (Fig. 3g, h). AWC has a transient odour-OFF response that peaks and then decays, and AIB has a sustained odour-OFF response, suggesting that it performs a temporal integration of AWC activity. AIY has an irregular odour-ON response, with short asynchronous events that are not well-represented in averaged traces.

AWC synapses are glutamate-mediated

AWC neurons have small clear vesicles at their synapses, suggesting the use of a small-molecule neurotransmitter[3]. *C. elegans eat-4(ky5)* mutants are defective in a vesicular glutamate transporter that concentrates glutamate into synaptic vesicles, and are defective in olfactory chemotaxis, local search and numerous other behaviours[12,26]. An *eat-4* complementary DNA expressed from the AWC-selective *odr-3* promoter (*AWC::eat-4*) rescued chemotaxis of *eat-4(ky5)* mutants in odour gradients, suggesting that AWC uses glutamate as its transmitter (Fig. 4a). The transgene also partially restored *eat-4(ky5)* local search behaviour—the AWC-dependent turning behaviour observed in the first 15 min after animals are removed from food (Fig. 4b). In the *AWC::eat-4* transgenic animals, turns were appropriately suppressed in the presence of food and in the later dispersal period, indicating that glutamate from AWC neurons stimulates appropriate local search and not continuous turning behaviour[6]. These experiments indicate that AWC neurons can release glutamate to stimulate olfactory chemotaxis and local search.

Local search behaviour is a time-dependent, quantitative response to the removal of food odours, so this assay was used for detailed analysis of the circuit downstream of AWC neurons. *C. elegans* has four classes of glutamate receptors: AMPA (α-amino-3-hydroxy-5-methyl-4-isoxazole propionic acid)-type glutamate-gated cation channels (encoded by eight *glr* genes); NMDA (*N*-methyl-D-aspartate receptor)-type glutamate-gated cation channels (encoded by two *nmr* genes); metabotropic G-protein-coupled glutamate receptors (encoded by two *mgl* genes); and glutamate-gated chloride channels (encoded by 10–20 *glc/avr* genes)[27–30]. The AMPA-type receptor GLR-1 is expressed by AIB interneurons as well as command interneurons that control forward and backward locomotion[27,28], and *glr-1(n2461)* mutant animals have diminished local search behaviour[12] (Fig. 4c). The local search defect was rescued by expressing *glr-1* from a promoter expressed in AIB and AIZ interneurons, but not in the bulk of *glr-1*-expressing neurons[31] (Fig. 4c). AIZ interneurons have not been reported to express endogenous *glr-1*, so AIB interneurons are probably the relevant site of *glr-1* rescue. Ablating the AIB neurons in the transgenic strain eliminated rescue, consistent with reconstitution of AIB function by the transgene (Fig. 4c). Ablation of AIZ interneurons in the transgenic strain had the same moderate effect as ablating AIZ in the wild type, indicating that AIZ

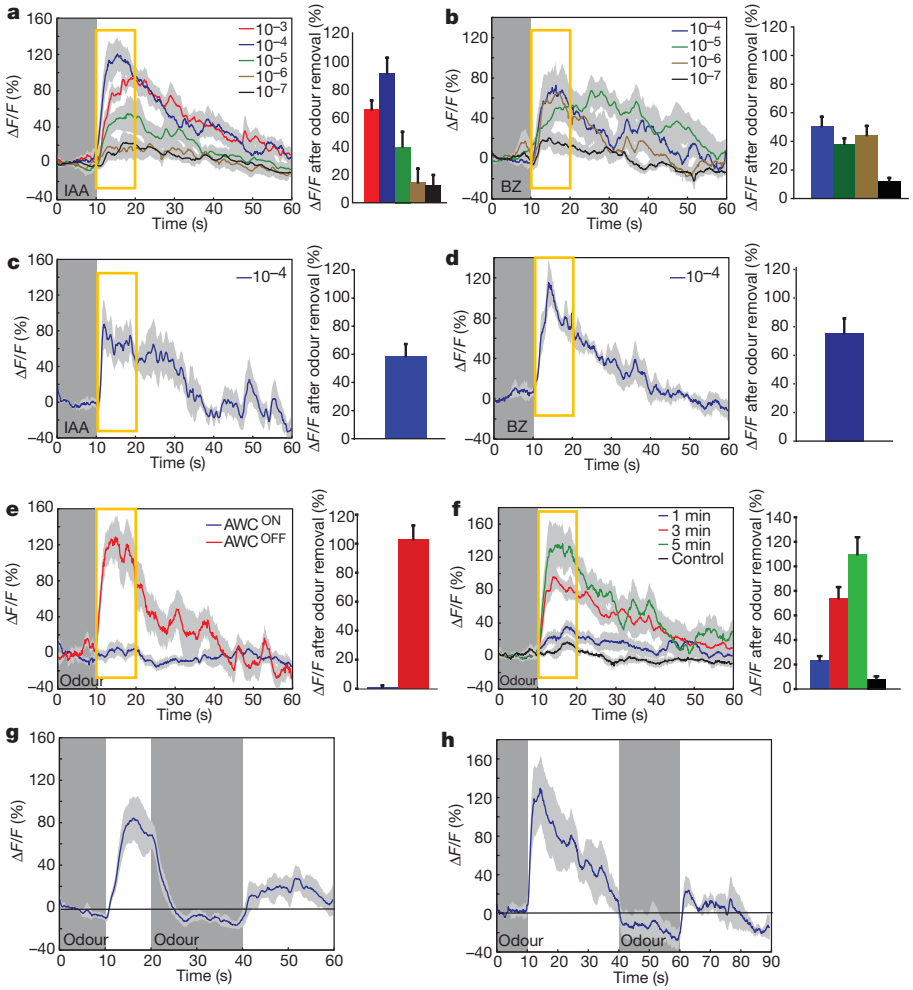

Figure 2 | Both classes of AWC neurons respond to odour removal. **a**–**d**, G-CaMP calcium responses of AWC^{ON} (**a**, **b**) or AWC^{OFF} (**c**, **d**) after removal from different concentrations of isoamyl alcohol (IAA; **a**, **c**) or benzaldehyde (BZ; **b**, **d**). **e**, Removal of 2,3-pentanedione activates AWC^{OFF}, but not AWC^{ON}. **f**, AWC^{ON} calcium responses in animals removed from isoamyl alcohol after different times of exposure. **g**, **h**, Secondary responses in AWC^{ON} after isoamyl alcohol was removed at 10 s, added back at 20 s (**g**) or 40 s (**h**), and then removed again 20 s later. Traces represent averages of 7–30 individual recordings (Supplementary Fig. 2). Bar graphs, average percentage change during the 10 s after odour removal (highlighted in yellow). Error bars and the shaded region around the curves represent s.e.m. The colour key for bar graphs is the same as that for the corresponding response curve.

function was not disrupted by ectopic *glr-1* expression (Fig. 4c and Supplementary Fig. 6d). These results indicate that AWC releases glutamate to stimulate *glr-1* on AIB interneurons. The *glr-1(n2461)* mutant defect is less severe than the defect caused by killing AIB, suggesting roles for additional glutamate receptors in AIB interneurons or glutamate-independent activity of AIB interneurons.

AIY neurons do not express excitatory *glr* or *nmr* genes, but do express the glutamate-gated chloride channel GLC-3 (refs 32 and 33). *glc-3(ok321)* mutants had diminished local search behaviour that was rescued by expressing *glc-3* from an AIY-specific promoter (Fig. 4d). Killing AIY interneurons results in the opposite effect—an amplified and long-lasting local search behaviour[14] (Supplementary Fig. 6d). These results indicate that AWC inhibits AIY during local search behaviour via glutamate release onto GLC-3. *glr-1(n2461);glc-3 (ok321)* double mutants were more defective than single mutants, consistent with parallel functions of AIB and AIY neurons (Fig. 4e).

To investigate this circuit model further, we used gain-of-function analysis in wild-type animals to test its predictions. In the vertebrate central nervous system, increased expression of synaptic AMPA-type glutamate receptors results in synaptic strengthening during long-term potentiation[34]. Building from this premise, we asked whether overexpression of glutamate receptors would strengthen behavioural connections between AWC, AIY and AIB neurons. Increased expression of *glc-3* from an AIY promoter or *glr-1* from an AIB promoter resulted in animals with increased turning during local search (Fig. 4f), as did overexpressing both *AIY::glc-3* and *AIB::glr-1* (Fig. 4g). Killing the AWC sensory neurons abolished these turning behaviours, indicating that the extra turns were evoked by sensory signals (Fig. 4g). Control experiments showed that misexpression of the AIB receptor in AIY interneurons and vice versa disrupted local search behaviour (Fig. 4h).

Calcium imaging of interneurons in mutants provided further evidence for glutamate-mediated signalling between AWC, AIB and AIY neurons. Neuronal calcium signals and local search behaviours are measured on different timescales (1 min versus >5 min, respectively), but results from both approaches were analogous. AIB calcium responses to odour removal were eliminated in animals lacking the vesicular glutamate transporter EAT-4, but were partially

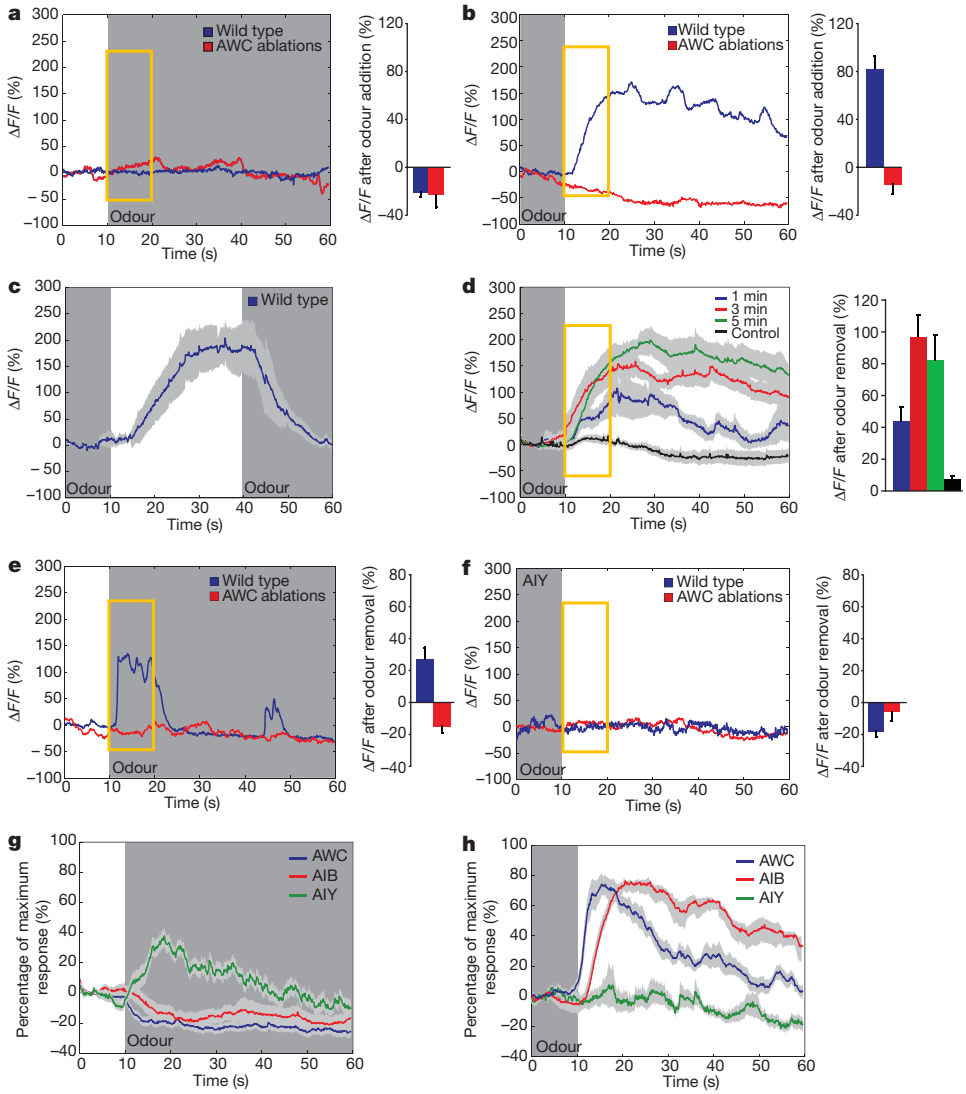

Figure 3 | Calcium responses in AIB and AIY interneurons. **a**, **b**, Representative and average calcium responses of AIB interneurons in wild-type and AWC-ablated animals on odour addition (**a**) or removal (**b**). Bar graphs, average percentage change during the 10 s after odour addition or removal (highlighted in yellow; $n = 22$ wild type, 7 AWC-ablated). **c**, Average AIB responses on odour removal (10 s) and re-addition (40 s). **d**, Average AIB responses to odour removal after different exposure times. **e**, **f**, Representative and average calcium responses of AIY neurites from wild-type and AWC-ablated animals on odour addition (**e**) or removal (**f**) ($n = 35$ wild type, 8 AWC-ablated). **g**, **h**, Averaged AWC^{ON} ($n = 30$), AIB ($n = 59$) and AIY ($n = 35$) responses, each trace normalized to its maximum response, on odour addition (**g**) and removal (**h**). Shading denotes the presence of odour. The shaded region around curves (**c**, **d**, **g** and **h**) indicates s.e.m. The colour key for bar graphs is the same as that for the corresponding response curve. Error bars indicate s.e.m.

restored by rescue of *eat-4* in AWC neurons (Fig. 5a, b). AIB responses were also eliminated in animals lacking the excitatory glutamate receptor GLR-1, and partially restored by rescue of *glr-1* in AIB neurons (Fig. 5c, d). The partial rescue may result from variable expression of transgenes, which is common in *C. elegans*, but it is likely that *eat-4* and *glr-1* also function in neurons other than AWC and AIB (for example, Supplementary Fig. 6b, c). The odour-induced increase in AIY calcium signals was eliminated in *glc-3(ok321)* mutant animals, supporting the identification of GLC-3 as an inhibitory postsynaptic receptor in AIY (Fig. 5e). However, in some animals (10 out of 22), an excitatory AIY calcium response was observed on odour removal (Fig. 5f and Supplementary Fig. 5e–h). These results indicate that AIY senses glutamate released from AWC neurons using the *glc-3* receptor and, in a *glc-3(ok321)* mutant background, may sense AWC signals through a second receptor with opposite activity.

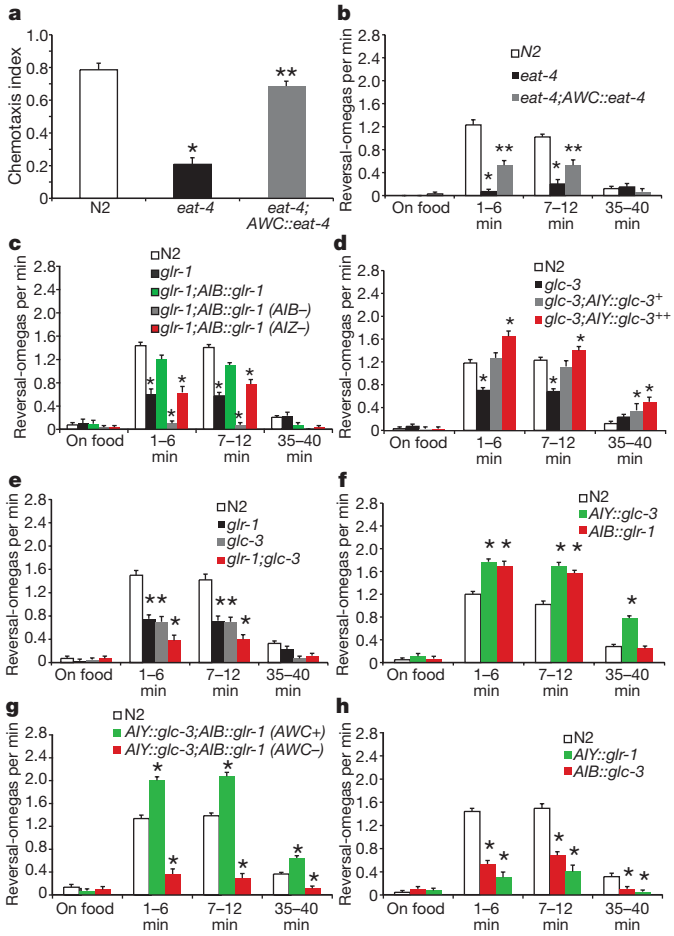

Figure 4 | AWC neurons signal through glutamate and glutamate receptors. **a**, **b**, AWC-selective expression of *eat-4* rescues chemotaxis to isoamyl alcohol (**a**) and partially rescues local search turning behaviour after removal from food (**b**). Co-expression of *eat-4* in ASK neurons enhances rescue (Supplementary Fig. 6). N2, wild-type control strain. **c**, Local search turning behaviour of *glr-1(n2461)* mutants, rescue by AIB expression of *glr-1*, and effects of cell ablation (AIB– and AIZ–). **d**, Local search turning behaviour of *glc-3*(ok321) animals and rescue by AIY expression of *glc-3*. Some transgenic lines have an overexpression phenotype (++). **e**, *glr-1(n2461);glc-3(ok321)* double mutants are more defective than either single mutant. **f**, Enhanced turning in AIB::GLR-1 and AIY::GLC-3 animals overexpressing glutamate receptors in wild-type background. **g**, Enhanced turning in AIY::GLC-3;AIB::GLR-1 double-transgenic animals, and effects of AWC ablations (AWC–). **h**, Decreased turning in animals misexpressing *glr-1* in AIY or *glc-3* in AIB. Reversal-omega, paired reversal-omega turning sequences. Error bars indicate s.e.m. One asterisk, different from N2; two asterisks, different from *eat-4* ($P < 0.05$, Bonferroni *t*-test).

Together, these results indicate that, when AWC is active, it releases glutamate that acts on GLR-1 at the AWC::AIB synapse and GLC-3 at the AWC::AIY synapse, resulting in activation of AIB and inhibition of AIY. Because cell ablations indicate that AIB promotes turns and AIY inhibits turns during local search[13,14] (Supplementary Fig. 6d), both functions of AWC glutamate should promote turning.

Odour removal evokes turning behaviour

Food is a complex stimulus, and, although local search behaviour is highly dependent on AWC activity, it also includes contributions from other sensory neurons[12–14]. To tighten the correlation between odour responses observed by calcium imaging and turning behaviour elicited by AWC neurons, we asked whether removal of the AWC-sensed odour isoamyl alcohol stimulated turning. These experiments were inspired by the observation that chemotaxis to attractive salts in *C. elegans* is associated with regulated turning behaviour[11,35]. The turning behaviour of freely moving animals was monitored in a small chamber that was rapidly shifted between humidified air and humidified air equilibrated with the AWC-sensed odour isoamyl alcohol. Wild-type animals transiently increased turning when odour was removed, a response resembling local search behaviour, and transiently suppressed turning when odour was presented (Fig. 6a). These responses were diminished in *eat-4(ky5)* mutants with defective glutamate-mediated transmission, but were rescued by the expression of *eat-4* in AWC neurons (Fig. 6a). Enhanced turning after odour removal had a shorter duration than local search (2–5 min) but, like local search, it was impaired in *glr-1(n2461);glc-3(ok321)* glutamate receptor double mutants (Fig. 6b). These results suggest that *glr-1* and *glc-3* function in odour-regulated turning behaviour induced by AWC neurons.

The suppression of turning on odour addition was independent of *glr-1* and *glc-3*, yet dependent on *eat-4* in AWC neurons, indicating that additional glutamate receptors act downstream of AWC neurons. Similarly, chemotaxis in odour gradients requires *eat-4*, but was only slightly impaired in *glr-1(n2461);glc-3(ok321)* double mutants (data not shown). Many predicted *C. elegans* glutamate-receptor genes are uncharacterized, but the AMPA-like receptor genes *glr-2* and *glr-5* are expressed in AIB, and *glr-2* is expressed in AIA neurons, so these genes are candidates for additional components of the odour response[36].

Discussion

From these experiments, we infer that AWC olfactory neurons have basal activity in the absence of odour, are inhibited by odour, and are stimulated by odour removal. These graded properties resemble those of motor neurons in the nematode *Ascaris suum*, which are non-spiking, have tonic neurotransmitter release at rest, and respond to excitatory or inhibitory inputs with graded changes in membrane potential and transmitter release[24]. Thus, graded transmission may be a property of many nematode neurons.

The sensory responses of AWC neurons are similar to those of vertebrate rod and cone photoreceptors, which have tonic activity in the dark, are hyperpolarized by light, and are depolarized by the removal of light[37]. Like AWC neurons, photoreceptors are non-spiking and have graded glutamate release. Molecular analogies also link AWC neurons with vertebrate photoreceptors: their sensory transduction pathways rely on G-protein-coupled receptors, G_i-like proteins, receptor-type guanylate cyclases and cyclic GMP-gated channels[5,37], and their differentiation is controlled by Otx homeodomain proteins[38,39]. The synaptic connections between AWC, AIY and AIB neurons are also reminiscent of those between vertebrate photoreceptors and their targets, the ON and OFF bipolar cells[40] (Fig. 6c). In the retina, glutamate from photoreceptors is sensed by AMPA-type receptors on the OFF bipolar cell, a connection that is functionally and molecularly analogous to the AWC-to-AIB connection[41]. The vertebrate ON bipolar cell is inhibited by glutamate, as are AIY

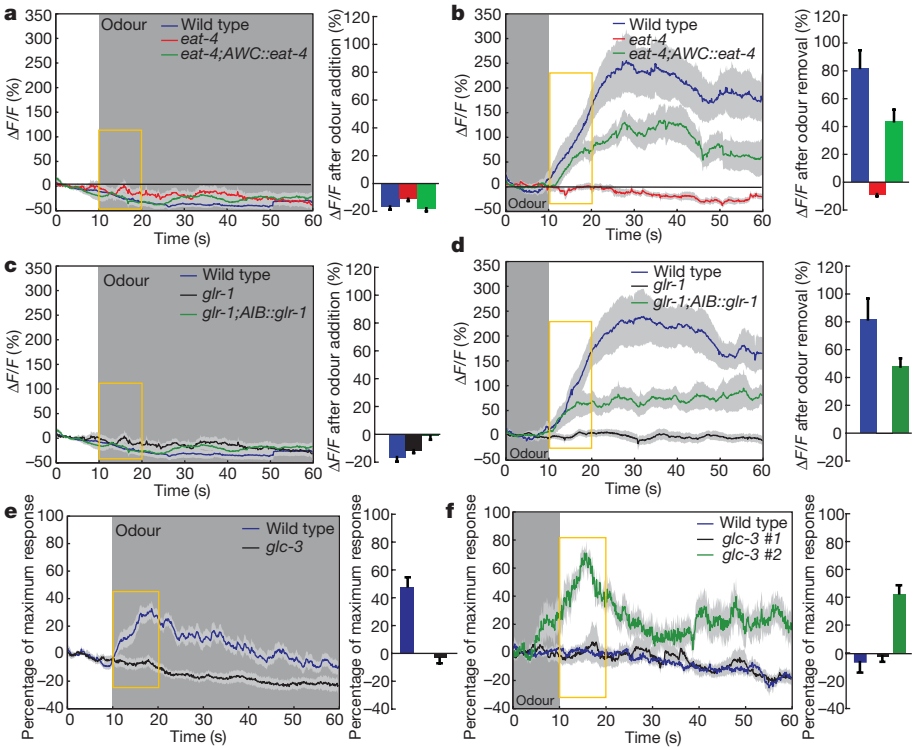

Figure 5 | AIB and AIY require different glutamate receptors. **a**, **b**, Calcium responses of AIB interneurons in wild type, *eat-4(ky5)* mutants, and *eat-4(ky-5)* mutants with an *AWC::eat-4* rescuing transgene on addition (**a**) or removal (**b**) of the odour isoamyl alcohol ($n = 12$ for each). **c**, **d**, Calcium responses of AIB interneurons in wild type, *glr-1(n2461)* mutants, and *glr-1(n2461)* mutants with an *AIB::glr-1* rescuing transgene on addition (**c**) or removal (**d**) of isoamyl alcohol ($n = 27$ for wild type, $n = 25$ for *glr-1*, $n = 12$ for *AIB::glr-1*). **e**, **f**, Calcium responses of AIY neurites in wild type and *glc-3(ok321)* mutants on addition (**e**) or removal (**f**) of odour ($n = 35$ for wild type, 22 for *glc-3*). Twelve out of 22 *glc-3(ok321)* mutants did not respond to odour (*glc-3*#1); 10 out of 22 *glc-3(ok321)* mutants responded to odour removal, unlike wild type (*glc-3*#2) (Supplementary Fig. 5). Shading denotes the presence of odour. Bar graphs, average percentage change during the 10 s after odour addition or removal (highlighted in yellow). Error bars and shaded regions around curves represent s.e.m. The colour key for bar graphs is the same as that for the corresponding response curve.

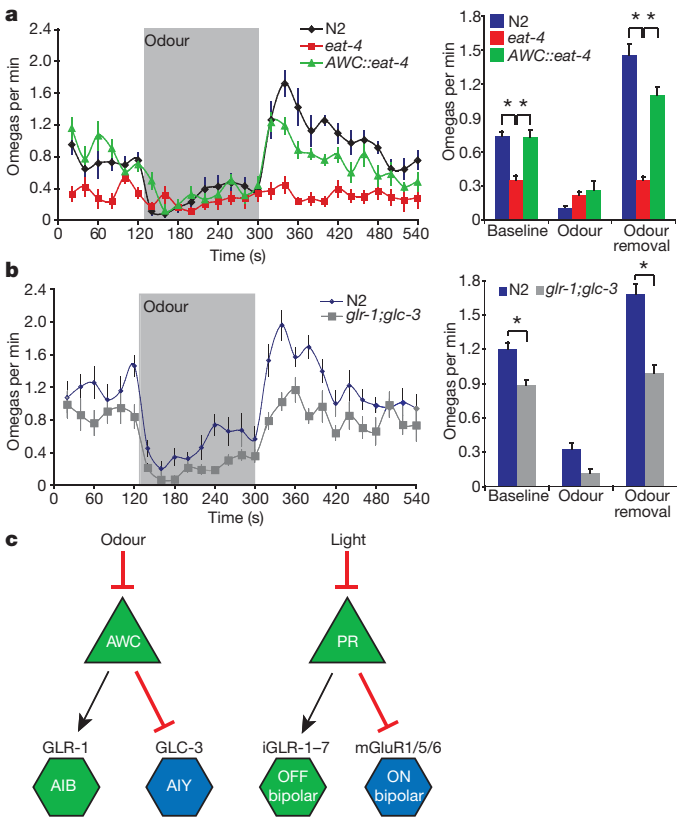

neurons. In mammals, the ON bipolar cell is inhibited by a G-protein-coupled glutamate receptor and, in fish, by a glutamate-gated chloride channel that is functionally although not molecularly similar to *C. elegans* GLC-3 (ref. 42). The parallel ON and OFF streams enhance contrast sensitivity in vertebrate vision[43]; it is possible that the parallel AIY and AIB neurons have analogous functions in odour detection.

Like AWC sensory neurons, AIB interneurons respond to odour removal, but, unlike the transient AWC calcium signals, AIB calcium responses are sustained for several minutes. These longer-lasting responses indicate that AIB interneurons integrate the AWC response over time (Supplementary Fig. 7). Persistent neural activity is a common feature of neural circuits, and can arise from cell-intrinsic or network mechanisms[23]. The persistent activity of AIB may contribute to sustained turning behaviour after odour or food removal.

Individual turns after odour removal are stochastic and infrequent; they are not synchronized to odour removal and AIB activation. This mismatch suggests that the AIB could be a gating neuron

Figure 6 | Odour-regulated turning behaviours. **a**, **b**, Omega turns of freely moving animals recorded before, during and after a 3-min pulse of the odour isoamyl alcohol ($t = 120$–300 s). Odour addition suppressed turns and odour removal enhanced turns in wild type N2 (Supplementary Fig. 6e, f). **a**, *eat-4(ky5)* mutants and rescue by AWC expression of *eat-4*. **b**, *glr-1(n2461);glc-3(ok321)* glutamate receptor double mutants. Bar graphs, omega turns during 1 min before odour addition (baseline), after odour addition and after odour removal. Asterisks, values different from *eat-4* (**a**) or wild type (**b**) at $P < 0.01$ (Bonferroni *t*-test). Error bars indicate s.e.m. **c**, Schematic comparing AWC, AIB and AIY neurons to vertebrate photoreceptors and bipolar neurons. iGluR, ionotropic glutamate receptor; mGluR, metabotropic glutamate receptor.

that facilitates turns, but does not trigger individual turning events[44]. The circuitry downstream of AIB interneurons may generate turns only when AIB is active and other unknown conditions are met. Possible sources for the turning signal are the secondary calcium transients in AWC neurons and the irregular, transient activity of AIY interneurons. Additional AWC target neurons such as AIA interneurons may also regulate turning; so far, the mechanism by which the AWC neuron suppresses turns on odour addition is unexplained, suggesting the existence of other target cells or receptors.

These experiments provide the beginnings of a circuit-level explanation for food-seeking behaviour in *C. elegans*. The regulation of turning by AWC neurons has features in common with the biased random walk, first described in bacterial chemotaxis and subsequently applied to *C. elegans* salt chemotaxis[11,45,46]. In this strategy, the animal senses temporal changes in attractant concentrations as it moves, resulting in long runs towards the attractant, short runs away from the attractant, and eventual accumulation at the point source. For AWC neurons, turning regulation can generate either chemotaxis or undirected local search; in both cases, turns are probabilistic and are not coupled tightly to stimuli. Our results and those of others suggest that the probabilistic turning circuit described here is both general and flexible. For example, temperature and salt stimuli affect *C. elegans* behaviour in a manner consistent with the biased random walk model[35,46–48], and the temperature-sensing and salt-sensing neurons synapse onto AIB, AIY, AIA and/or AIZ interneurons[3,25,49]. A serotonin receptor essential for olfactory learning acts in AIY, AIB and AIZ interneurons, suggesting that the circuit is subject to plasticity[50]. Further studies of the circuit should shed light on the mechanism for stochastic behaviours, the generation of persistent behavioural responses to transient stimuli, and temporal integration in the nervous system.

METHODS SUMMARY

Neuronal calcium responses were measured by detecting changes in fluorescence of G-CaMP, a non-ratiometric calcium indicator[16]; control experiments indicated that G-CaMP performed comparably to the ratiometric indicator cameleon in this system[19] (Supplementary Methods). Custom-designed microfluidic devices for trapping, stimulating and imaging calcium transients in *C. elegans* were fabricated from PDMS[19]. Fluid streams under laminar flow were used to deliver buffer or odour stimuli to the animal's nose, using flow by means of two alternative side-streams to control the delivery of stimuli without changing fluid pressure. Images were captured using a Coolsnap HQ camera and were analysed using Metamorph software.

Exploratory behaviours were scored essentially as described[14]. Animals were removed from food to a covered, food-free nematode growth medium (NGM) plate. Their behaviour was observed directly, and turning events were recorded using a Perl script. At least eight animals were scored blind for each condition.

Odour-induced turning responses were monitored in a custom-fabricated Plexiglass chamber over an agar surface, with an inlet, an outlet and a central imaging arena. Humidified air with or without odour was delivered to >20 freely moving animals using an electronic valve. Movies of these animals were analysed using automated tracking software, which is distributed at http://wormsense.stanford.edu/tracker. The software automatically identifies tens of animals, computes and tracks the centroid of each animal, and identifies turns on the basis of changes in angular velocity (see Supplementary Methods).

Full Methods and any associated references are available in the online version of the paper at www.nature.com/nature.

Received 14 August; accepted 24 September 2007.

1. Milo, R. *et al.* Network motifs: simple building blocks of complex networks. *Science* **298,** 824–827 (2002).
2. Chalfie, M. *et al.* The neural circuit for touch sensitivity in *Caenorhabditis elegans*. *J. Neurosci.* **5,** 956–964 (1985).
3. White, J. G., Southgate, E., Thomson, J. N. & Brenner, S. The structure of the nervous system of the nematode *Caenorhabditis elegans*. *Phil. Trans. R. Soc. Lond. B* **314,** 1–340 (1986).
4. de Bono, M. & Maricq, A. V. Neuronal substrates of complex behaviors in *C. elegans*. *Annu. Rev. Neurosci.* **28,** 451–501 (2005).
5. Bargmann, C. I. in *Wormbook* (ed. The *C. elegans* Research Community) WormBook doi/10.1895/wormbook.1.123. 1 ⟨http://www.wormbook.org⟩ (2006).
6. Zheng, Y., Brockie, P. J., Mellem, J. E., Madsen, D. M. & Maricq, A. V. Neuronal control of locomotion in *C. elegans* is modified by a dominant mutation in the GLR-1 ionotropic glutamate receptor. *Neuron* **24,** 347–361 (1999).
7. Tobin, D. *et al.* Combinatorial expression of TRPV channel proteins defines their sensory functions and subcellular localization in *C. elegans* neurons. *Neuron* **35,** 307–318 (2002).
8. Goodman, M. B., Hall, D. H., Avery, L. & Lockery, S. R. Active currents regulate sensitivity and dynamic range in *C. elegans* neurons. *Neuron* **20,** 763–772 (1998).
9. Kerr, R. *et al.* Optical imaging of calcium transients in neurons and pharyngeal muscle of *C. elegans*. *Neuron* **26,** 583–594 (2000).
10. Mellem, J. E., Brockie, P. J., Zheng, Y., Madsen, D. M. & Maricq, A. V. Decoding of polymodal sensory stimuli by postsynaptic glutamate receptors in *C. elegans*. *Neuron* **36,** 933–944 (2002).
11. Pierce-Shimomura, J. T., Morse, T. M. & Lockery, S. R. The fundamental role of pirouettes in *Caenorhabditis elegans* chemotaxis. *J. Neurosci.* **19,** 9557–9569 (1999).
12. Hills, T., Brockie, P. J. & Maricq, A. V. Dopamine and glutamate control area-restricted search behavior in *Caenorhabditis elegans*. *J. Neurosci.* **24,** 1217–1225 (2004).
13. Wakabayashi, T., Kitagawa, I. & Shingai, R. Neurons regulating the duration of forward locomotion in *Caenorhabditis elegans*. *Neurosci. Res.* **50,** 103–111 (2004).
14. Gray, J. M., Hill, J. J. & Bargmann, C. I. A circuit for navigation in *Caenorhabditis elegans*. *Proc. Natl Acad. Sci. USA* **102,** 3184–3191 (2005).
15. Zhao, B., Khare, P., Feldman, L. & Dent, J. A. Reversal frequency in *Caenorhabditis elegans* represents an integrated response to the state of the animal and its environment. *J. Neurosci.* **23,** 5319–5328 (2003).
16. Nakai, J., Ohkura, M. & Imoto, K. A high signal-to-noise Ca^{2+} probe composed of a single green fluorescent protein. *Nature Biotechnol.* **19,** 137–141 (2001).
17. Pologruto, T. A., Yasuda, R. & Svoboda, K. Monitoring neural activity and [Ca^{2+}] with genetically encoded Ca^{2+} indicators. *J. Neurosci.* **24,** 9572–9579 (2004).
18. Jospin, M., Jacquemond, V., Mariol, M. C., Segalat, L. & Allard, B. The L-type voltage-dependent Ca^{2+} channel EGL-19 controls body wall muscle function in *Caenorhabditis elegans*. *J. Cell Biol.* **159,** 337–348 (2002).
19. Chronis, N., Zimmer, M. & Bargmann, C. I. Microfluidics for *in vivo* imaging of neuronal and behavioral activity in *Caenorhabditis elegans*. *Nature Methods* **4,** 727–731 (2007).
20. Bargmann, C. I., Hartwieg, E. & Horvitz, H. R. Odorant-selective genes and neurons mediate olfaction in *C. elegans*. *Cell* **74,** 515–527 (1993).
21. Colbert, H. A. & Bargmann, C. I. Environmental signals modulate olfactory acuity, discrimination, and memory in *Caenorhabditis elegans*. *Learn. Mem.* **4,** 179–191 (1997).
22. Wes, P. D. & Bargmann, C. I. C. *elegans* odour discrimination requires asymmetric diversity in olfactory neurons. *Nature* **410,** 698–701 (2001).
23. Major, G. & Tank, D. Persistent neural activity: prevalence and mechanisms. *Curr. Opin. Neurobiol.* **14,** 675–684 (2004).
24. Davis, R. E. & Stretton, A. O. W. Signalling properties of *Ascaris* motor neurons: graded synaptic transmission and tonic transmitter release. *J. Neurosci.* **9,** 415–425 (1989).
25. Clark, D. A., Biron, D., Sengupta, P. & Samuel, A. D. The AFD sensory neurons encode multiple functions underlying thermotactic behavior in *Caenorhabditis elegans*. *J. Neurosci.* **26,** 7444–7451 (2006).
26. Lee, R. Y., Sawin, E. R., Chalfie, M., Horvitz, H. R. & Avery, L. EAT-4, a homolog of a mammalian sodium-dependent inorganic phosphate cotransporter, is necessary for glutamatergic neurotransmission in *Caenorhabditis elegans*. *J. Neurosci.* **19,** 159–167 (1999).
27. Hart, A. C., Sims, S. & Kaplan, J. M. Synaptic code for sensory modalities revealed by *C. elegans* GLR-1 glutamate receptor. *Nature* **378,** 82–85 (1995).
28. Maricq, A. V., Peckol, E., Driscoll, M. & Bargmann, C. I. Mechanosensory signalling in *C. elegans* mediated by the GLR-1 glutamate receptor. *Nature* **378,** 78–81 (1995).
29. Cully, D. F. *et al.* Cloning of an avermectin-sensitive glutamate-gated chloride channel from *Caenorhabditis elegans*. *Nature* **371,** 707–711 (1994).
30. Dillon, J., Hopper, N. A., Holden-Dye, L. & O'Connor, V. Molecular characterization of the metabotropic glutamate receptor family in *Caenorhabditis elegans*. *Biochem. Soc. Trans.* **34,** 942–948 (2006).
31. Chou, J. H., Bargmann, C. I. & Sengupta, P. The *Caenorhabditis elegans odr-2* gene encodes a novel Ly-6-related protein required for olfaction. *Genetics* **157,** 211–224 (2001).
32. Horoszok, L., Raymond, V., Sattelle, D. B. & Wolstenholme, A. J. GLC-3: a novel fipronil and BIDN-sensitive, but picrotoxin-insensitive, L-glutamate-gated chloride channel subunit from *Caenorhabditis elegans*. *Br. J. Pharmacol.* **132,** 1247–1254 (2001).
33. Wenick, A. S. & Hobert, O. Genomic *cis*-regulatory architecture and *trans*-acting regulators of a single interneuron-specific gene battery in *C. elegans*. *Dev. Cell* **6,** 757–770 (2004).
34. Malinow, R. & Malenka, R. C. AMPA receptor trafficking and synaptic plasticity. *Annu. Rev. Neurosci.* **25,** 103–126 (2002).
35. Miller, A. C., Thiele, T. R., Faumont, S., Moravec, M. L. & Lockery, S. R. Step-response analysis of chemotaxis in *Caenorhabditis elegans*. *J. Neurosci.* **25,** 3369–3378 (2005).
36. Brockie, P. J., Madsen, D. M., Zheng, Y., Mellem, J. & Maricq, A. V. Differential expression of glutamate receptor subunits in the nervous system of

Caenorhabditis elegans and their regulation by the homeodomain protein UNC-42. *J. Neurosci.* **21,** 1510–1522 (2001).
37. Zhang, X. & Cote, R. H. cGMP signaling in vertebrate retinal photoreceptor cells. *Front. Biosci.* **10,** 1191–1204 (2005).
38. Furukawa, T., Morrow, E. M. & Cepko, C. L. *Crx*, a novel otx-like homeobox gene, shows photoreceptor-specific expression and regulates photoreceptor differentiation. *Cell* **91,** 531–541 (1997).
39. Lanjuin, A., VanHoven, M. K., Bargmann, C. I., Thompson, J. K. & Sengupta, P. *Otx/otd* homeobox genes specify distinct sensory neuron identities in *C. elegans*. *Dev. Cell* **5,** 621–633 (2003).
40. Yang, X.-L. Characterization of receptors for glutamate and GABA in retinal neurons. *Prog. Neurobiol.* **73,** 127–150 (2004).
41. Wassle, H. Parallel processing in the mammalian retina. *Nature Rev. Neurosci.* **5,** 747–757 (2004).
42. Grant, G. B. & Dowling, J. E. A glutamate-activated chloride current in cone-driven ON bipolar cells of the white Perch retina. *J. Neurosci.* **15,** 3852–3862 (1995).
43. Schiller, P. H., Sandell, J. H. & Maunsell, J. H. Functions of the ON and OFF channels of the visual system. *Nature* **322,** 824–825 (1986).
44. Taha, S. A. & Fields, H. L. Inhibitions of nucleus accumbens neurons encode a gating signal for reward-directed behavior. *J. Neurosci.* **26,** 217–222 (2006).
45. Berg, H. C. & Brown, D. A. Chemotaxis in *Escherichia coli* analysed by three-dimensional tracking. *Nature* **239,** 500–504 (1972).
46. Dusenbery, D. B. Responses of the nematode *Caenorhabditis elegans* to controlled chemical stimulation. *J. Comp. Physiol.* **136,** 327–331 (1980).
47. Ryu, W. S. & Samuel, A. D. Thermotaxis in *Caenorhabditis elegans* analyzed by measuring responses to defined thermal stimuli. *J. Neurosci.* **22,** 5727–5733 (2002).
48. Zariwala, H. A., Miller, A. C., Faumont, S. & Lockery, S. R. Step response analysis of thermotaxis in *Caenorhabditis elegans*. *J. Neurosci.* **23,** 4369–4377 (2003).
49. Mori, I. & Ohshima, Y. Neural regulation of thermotaxis in *Caenorhabditis elegans*. *Nature* **376,** 344–348 (1995).
50. Zhang, Y., Lu, H. & Bargmann, C. I. Pathogenic bacteria induce aversive olfactory learning in *Caenorhabditis elegans*. *Nature* **438,** 179–184 (2005).

Supplementary Information is linked to the online version of the paper at www.nature.com/nature.

Acknowledgements We thank the *C. elegans* Knockout Consortium and the *Caenorhabditis* Genetic Center (CGC) for strains, A. Wolstenholme for the *glc-3* cDNA, P. Sengupta for the *srsx-3* promoter, and M. Meister, M. Zimmer, B. Snyder, G. Lee, D. Albrecht, M. Hilliard and other Bargmann laboratory members for critical help, insights and advice. S.H.C. was supported by the Damon Runyon Cancer Research Foundation and C.I.B. is an Investigator of the Howard Hughes Medical Institute. This work was supported by the Howard Hughes Medical Institute (C.I.B.) and the Klingenstein Fund for Neuroscience (M.B.G.).

Author Contributions S.H.C. designed and performed experiments, analysed data and wrote the paper; N.C., M.T. and J.M.G. designed and performed experiments; D.R. and M.B.G. developed analytical tools; and C.I.B. designed experiments, analysed data and wrote the paper.

Author Information Reprints and permissions information is available at www.nature.com/reprints. Correspondence and requests for materials should be addressed to C.I.B. (cori@rockefeller.edu).

METHODS

Calcium imaging. The microfluidic device was fabricated using standard micromachining procedures[19,51]. The design was drawn in Autocad and the chrome mask was generated by a mask-making service (Microlab, University of California, Berkeley). A master mould was created by spin casting (~2,800 r.p.m.) and photolithographically patterning a 28-μm-thick layer of SU-8-2025 photoresist on a bare silicon wafer. A PDMS prepolymer mixture (Sylgard 184, 10:1) was cast over the mould and cured on a hot plate for 2 h at 70 °C. PDMS devices were peeled off the mould, treated with air plasma (30 W for 30 s) and irreversibly bonded to a glass coverslip. A sharpened needle (0.16 inch inner diameter × 0.25 inch outer diameter) was used to create inlets and outlets for the PDMS chip. Syringes with buffers were connected to the microfluidic device using polyethylene tubing (0.58 mm inner diameter × 0.95 mm outer diameter). Constant suction applied to the outlet of the chip generated laminar flow profiles for the four different streams (two dye (fluorescein) streams, one buffer stream and one stimulus stream). Individual worms were sucked into a buffer-filled polyethylene tube with the aid of a syringe and injected into the entrance of the chip by manually increasing the pressure by means of the syringe. A three-way valve (The Lee Company, 778360) regulated the two dye streams allowing only one dye stream into the chip at any given time. In the OFF condition (Fig. 1c, channels 1–3 open), the dye stream (flow 1) pushed the stimulus away from the nose, immersing the nose in the buffer stream (flow 2). In the ON condition (Fig. 1d, channels 2–4 open), dye stream 4 pushed stimulus stream 3 (odour or bacterial-conditioned medium of A_{600} 1.0 in buffer) towards the nose of the trapped animal. Indirect control of fluid streams was necessary because AWC neurons respond strongly to small changes in fluid pressure (data not shown). G-CaMP imaging was performed on a Zeiss Axioscope upright microscope using a Coolsnap HQ photometrics camera. A detailed description of image analysis is provided in the Supplementary Methods.

Odour flow assays. A custom-fabricated Plexiglass device with an inlet, an outlet and a central arena (30 mm × 44 mm wide and 0.3 mm high; air volume 3.6 ml) was placed on a food-free NGM assay plate to create a chamber for imaging movement. Animals were picked on the NGM plate and corralled in the arena with a filter paper soaked in the repellent copper chloride (20 mM $CuCl_2$), which kept them in view for 30 min. The inlet was controlled by two three-way valves (The Lee Company, 778360) allowing air equilibrated in water or air equilibrated in isoamyl alcohol diluted in water to flow through the chamber at 200 ml min^{-1}. The saturated vapour concentration of isoamyl alcohol is 1.2×10^{-4} M at 20 °C, corresponding to a 10^{-5} dilution in liquid phase. Stimulus-equilibrated air was further diluted 1:10 in air before being presented to the behaviour chamber. A Zeiss dissecting microscope and a Macrofire SDK camera captured the behaviour of all animals. Images were analysed using an automatic tracking system (see Supplementary Methods). Results were averaged in 20-s bins.

Quantitative analysis of exploratory behaviour. Animals were scored for exploratory behaviour on food, immediately after removal from food, and at long times off food. Adult animals were first observed and scored for 5 min on a lawn of OP50 *Escherichia coli* bacteria on an NGM plate and then transferred to a food-free NGM plate, where they were observed and scored during 15 of the next 40 min. The assay was performed as described[14] except that the food-free assay plate was covered by a lid during the assay. All turns and reversals were scored by eye, by an investigator blind to the genotype and ablation status of the animal. Reversals that had three or more head swings were identified as long reversals; these are essentially absent in the presence of food (Supplementary Fig. 6a, b)[14]. Turns in which the head nearly touched the tail or turns in which a single head swing led to a reorientation of more than 135° were identified as omega turns (Supplementary Fig. 6a)[14]. Results in Fig. 4 are reported as RevOmega values, which represent coupled large reversal-omega pairs, but qualitatively similar results were obtained when either large reversals or omega turns were scored individually (Supplementary Table 1). Reversals coupled to omega turns were chosen for display because of their consistency in wild-type animals across various experiments. Data were analysed using Perl scripts to calculate reversal and omega frequencies.

51. Younan, X. & Whitesides, G. Soft lithography. *Ann. Rev. Mater. Sci.* **28**, 153–184 (1998).

CORRIGENDUM

doi:10.1038/nature06540

Dissecting a circuit for olfactory behaviour in *Caenorhabditis elegans*

Sreekanth H. Chalasani, Nikos Chronis, Makoto Tsunozaki, Jesse M. Gray, Daniel Ramot, Miriam B. Goodman & Cornelia I. Bargmann

Nature 450, 63–70 (2007)

In parts of Fig. 5c and e of this Article, incorrect data were inadvertently used. The corrected figure panels are shown below. Our results and conclusions are not affected.

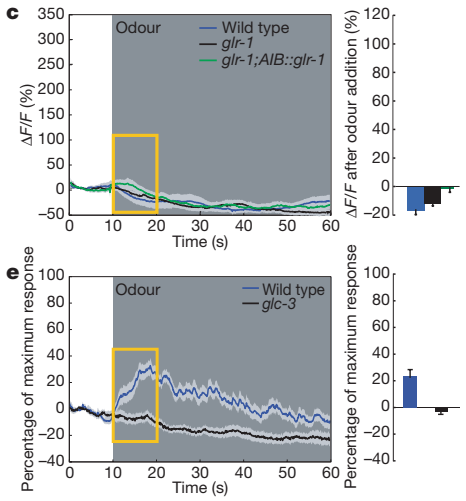

CORRIGENDUM

doi:10.1038/nature06541

Gene-specific control of inflammation by TLR-induced chromatin modifications

Simmie L. Foster, Diana C. Hargreaves & Ruslan Medzhitov

Nature 447, 972–978 (2007)

A citation (ref. 1) was inadvertently removed during revision of this Article, which also emphasized the potential importance of chromatin modifications in innate immune responses.

1. Chan, C., Li, L., McCall, C. E. & Yoza, B. Endotoxin tolerance disrupts chromatin remodeling and NF-κB transactivation at the IL-1β promoter. *J. Immunol.* 175, 461–468 (2005).